

## Magnetic force microscopy of helical states in multilayer nanomagnets

A. A. Fraerman,<sup>1</sup> B. A. Gribkov,<sup>1</sup> S. A. Gusev,<sup>1</sup> A. Yu. Klimov,<sup>1</sup> V. L. Mironov,<sup>1,a)</sup>  
D. S. Nikitushkin,<sup>1</sup> V. V. Rogov,<sup>1</sup> S. N. Vdovichev,<sup>1</sup> B. Hjorvarsson,<sup>2</sup> and H. Zabel<sup>3</sup>

<sup>1</sup>*Institute for Physics of Microstructures RAS, Nizhny Novgorod 603950, Russia*

<sup>2</sup>*Department of Physics, Uppsala University, SE-75121 Uppsala, Sweden*

<sup>3</sup>*Institut für Experimentalphysik/Festkörperphysik, Ruhr-Universität Bochum, D-44780 Bochum, Germany*

(Received 23 November 2007; accepted 24 January 2008; published online 8 April 2008)

We have used magnetic force microscopy (MFM) to investigate noncollinear helical states in multilayer nanomagnets, consisting of a stack of single domain ferromagnetic disks separated by insulating nonmagnetic spacers. The nanomagnets were fabricated from a [Co/Si]×3 multilayer thin film structure by electron beam lithography and ion beam etching. The structural parameters (Co layer and spacer thicknesses) were optimized to obtain a clear spiral signature in the MFM contrast, taking into account the magnetostatic interaction between the layers. MFM contrast corresponding to the helical states with different helicities was observed for the optimized structure with Co layer thicknesses of 16, 11, and 8 nm, and with 3 nm Si spacer thickness. © 2008 American Institute of Physics. [DOI: 10.1063/1.2903136]

### INTRODUCTION

The discoveries of giant (tunnel) magnetoresistance<sup>1–4</sup> and spin transfer<sup>5</sup> in ferromagnetic metallic multilayers significantly contributed to our understanding of charge and spin transport in ferromagnets and has led to important applications such as memory devices and sensors. Studies of the magnetoresistance of magnetic multilayers have generally concentrated on the differences between the conductivity of parallel and antiparallel magnetizations of the layers. Coupling of spin and orbital degrees of freedom in noncollinear magnetic systems are almost completely unexplored. The recent interest in the transport properties of non collinear magnetizations was stimulated by the spin-transfer torque effect.<sup>6–12</sup> There are different approaches for obtaining noncollinear magnetization distributions such as domain walls,<sup>13</sup> magnetic springs,<sup>14</sup> as well as helical magnetic states in natural crystals.<sup>15,16</sup> However, the control and manipulation of noncollinear magnetization in such structures is rather limited. Here, we will show that noncollinear magnetic structures can be realized in artificial multilayer nanomagnets. The resulting helical structure is verified by magnetic force microscopy.

### THEORETICAL CONSIDERATION

Helical states in multilayer nanomagnets can be obtained through the magnetostatic interaction, using the right choice of parameters. The strength and sign of the interaction energy for two uniformly magnetized particles are determined by the mutual orientation of their total magnetic moments. For example, when two ferromagnetic disks are separated by a nonmagnetic spacer, the magnetostatic interaction leads to an antiferromagnetic (AF) orientation of their magnetization with respect to each other. The situation is significantly changed when the stack consists of three magnetic layers. The interaction between disks leads to frustration in the mag-

netic moments orientation for the first and third disks. If the interaction between these disks is large enough and if the magnetic moments are confined and free to rotate in the plane, the ground state of this system is noncollinear (Fig. 1).

Taking into account only the magnetostatic interaction, the energy of the system of three uniformly magnetized circular disks can be represented as

$$E = \varepsilon_{21} \cos \theta_{21} + \varepsilon_{23} \cos \theta_{23} + \varepsilon_{13} \cos \theta_{13}, \quad (1)$$

where  $\varepsilon_{ij}$  ( $i, j=1, 2$ , and  $3$ ) are the interaction energies between  $i$  and  $j$  disks ( $\varepsilon_{ij} > 0$ ), and  $\theta_{ij}$  are the angles between the magnetic moment directions in the  $i$  and  $j$  disks relative to the direction of the magnetic moment in the second layer. In a system with three identical magnetic disks and identical spacer thicknesses,  $\varepsilon_{21} = \varepsilon_{23} = \varepsilon$ . In this case, varying expression (1), we obtain that a minimum of the magnetostatic energy is realized for  $\theta_{21} = \theta_{23} = \theta$ . The angle  $\theta$  is defined by one of the following equations:

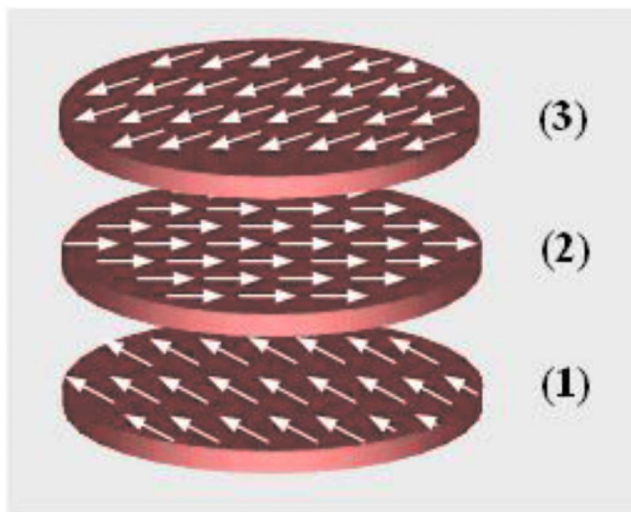


FIG. 1. (Color online) Noncollinear helical magnetic state in the three single-domain disks system.

<sup>a)</sup>Electronic mail: mironov@ipm.sci-nnov.ru

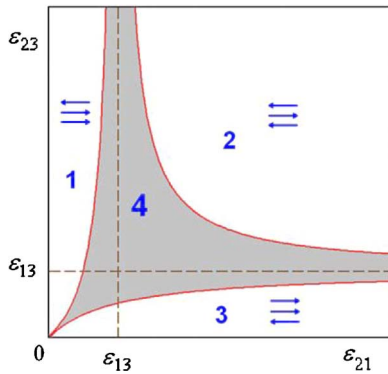


FIG. 2. (Color online) The diagram of states in triple nanodisk. The central region 4 (indicated in gray color) corresponds to the noncollinear states.

$$\sin \theta = 0, \quad (2)$$

$$\cos \theta = -\frac{\varepsilon}{2\varepsilon_{13}}. \quad (3)$$

Thus, if the interaction energy of the next nearest neighbors is small, i.e.,  $2\varepsilon_{13} < \varepsilon$ , then an AF ordered (antiparallel) state ( $\theta = \pi$ ) is formed. However, for  $2\varepsilon_{13} > \varepsilon$ , a noncollinear magnetic spiral state (Fig. 1) is predicted.

The noncollinear state can also be obtained in a stack consisting of ferromagnetic layers with unequal thicknesses. In this case,  $\varepsilon_{21} \neq \varepsilon_{23} \neq \varepsilon_{13}$ . The magnitudes of  $\varepsilon_{ij}$  depend on the diameter and the thickness of the ferromagnetic disks as well as on the spacer layer thickness. The generalized phase diagram of triple nanodisks is represented in Fig. 2.

Depending on the ratio between  $\varepsilon_{21}$ ,  $\varepsilon_{23}$ , and  $\varepsilon_{13}$ , both collinear (regions 1, 2, and 3 in Fig. 2) and noncollinear (region 4) states can be obtained in triple nanodisks. The lines separating the regions with different states are defined by the following equations:

$$\varepsilon_{23} = \frac{\varepsilon_{21}\varepsilon_{13}}{\varepsilon_{13} - \varepsilon_{21}}, \quad \varepsilon_{23} = \frac{\varepsilon_{21}\varepsilon_{13}}{\varepsilon_{21} - \varepsilon_{13}}, \quad \varepsilon_{23} = \frac{\varepsilon_{21}\varepsilon_{13}}{\varepsilon_{21} + \varepsilon_{13}}. \quad (4)$$

In the noncollinear state, the angles  $\theta_{21}$  and  $\theta_{23}$  between the magnetic moments in neighboring layers are defined as

$$\cos \theta_{21} = \frac{\varepsilon_{13}^2 \varepsilon_{23}^2 - \varepsilon_{21}^2 \varepsilon_{23}^2 - \varepsilon_{13}^2 \varepsilon_{21}^2}{2\varepsilon_{21}^2 \varepsilon_{23} \varepsilon_{13}},$$

$$\cos \theta_{23} = \frac{\varepsilon_{21}^2 \varepsilon_{13}^2 - \varepsilon_{21}^2 \varepsilon_{23}^2 - \varepsilon_{13}^2 \varepsilon_{23}^2}{2\varepsilon_{21} \varepsilon_{23}^2 \varepsilon_{13}}. \quad (5)$$

In particular, for the point of asymptotic intersection ( $\varepsilon_{21} = \varepsilon_{23} = \varepsilon_{13}$ ), the angles are  $\theta_{21} = 240^\circ$ ,  $\theta_{23} = 120^\circ$  for “right” hand helicoids and  $\theta_{21} = 120^\circ$ ,  $\theta_{23} = 240^\circ$  for “left” hand helicoids. Note that the spiral state is doubly degenerate, i.e., the energies for left and right helicoids are identical.

The analytical calculations based on minimization of the magnetostatic energy are in good agreement with computer simulations (based on Landau–Lifshitz–Gilbert equations) of the magnetic states for the same triple nanodisks. The discrepancy in the values of  $\theta_{21}$  and  $\theta_{23}$  calculated by these two methods are not more than 2%.

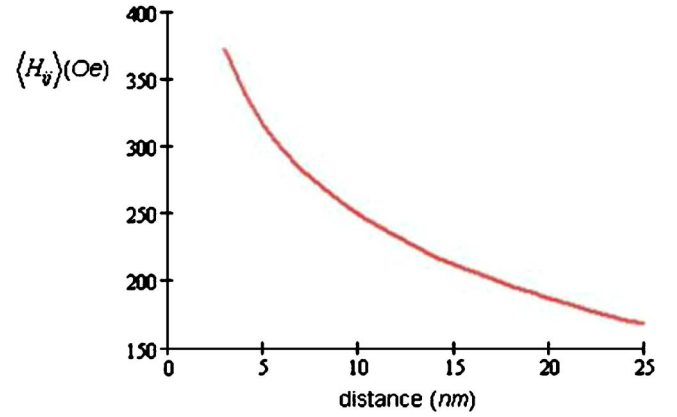


FIG. 3. (Color online) Dependence of volume averaged longitudinal component of the magnetic field with the distance between the disks  $z_{ij}$ .

Thus, the main factor determining the presence of noncollinear ordering is the ratio of the interaction between the nearest and the next nearest neighbor disks. Taking into account the cylindrical symmetry of the stacked disks and the homogeneity of the magnetization, the energy of the magnetostatic interaction between the disks can be obtained by

$$\varepsilon_{ij}(|z_i - z_j|) = M_s V \langle H_{ij} \rangle, \quad (6)$$

where  $M_s$  is saturation magnetization,  $V$  is the disk volume,  $z_i$  and  $z_j$  are the coordinates for the center of disk  $i$  and disk  $j$ , respectively, and  $\langle H_{ij} \rangle$  is the volume averaged longitudinal (parallel to the magnetization direction) component of the magnetic field induced by disk  $i$  within disk  $j$ . The results of numerical micromagnetic calculations of the dependence of  $\langle H_{ij} \rangle$  on the distance  $z_{ij} = |z_i - z_j|$  for Co disks ( $M_s = 1400$  G) with a diameter of 300 nm and a height of 5 nm are shown in Fig. 3.

When the Co layers in nanomagnets are separated by a 3 nm thick nonmagnetic spacer, the ratio  $\varepsilon/\varepsilon_{13}$  is about 1.25. Thus, using only the magnetostatic interaction between the disks, a helical state with an angular displacement close to  $2\pi/3$  is expected. In contrast to natural helimagnets such as Ho or Dy, the spiral state for three magnetic nanodisks is solely caused by the competition between nearest and next nearest neighbor interactions. Since the magnetostatic interaction for such disks is rather strong ( $\varepsilon_{13} \sim 10^{-10} - 10^{-11}$  erg), the helical state should be stable at room temperature.

## SAMPLE PREPARATION AND EXPERIMENTAL TECHNIQUE

The [Co/Si] $\times$ 3 multilayer was grown using magnetron sputtering. The film thicknesses of the layers were analyzed by x-ray reflectometry and the magnetic properties of the multilayer were determined by the magneto-optical Kerr effect. The coercivity of the ferromagnetic Co films did not exceed 20 Oe. Si layers were used as spacer layers, effectively hindering any interaction between the Co layers except the magnetostatic interaction. The multilayers were patterned using electron beam lithography and ion beam etching. The details of the lithographic processes are described in Ref. 17. The Co disks had diameters of 300 nm and thicknesses of

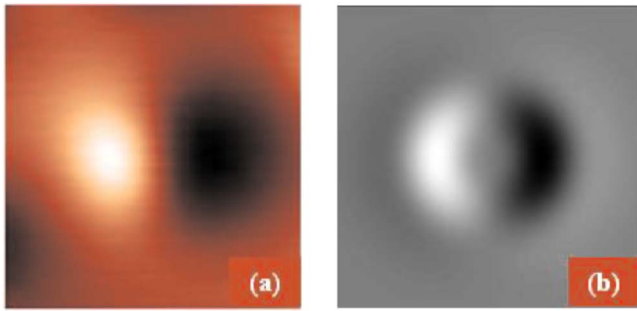


FIG. 4. (Color online) (a) Experimental and (b) simulated MFM contrast distributions for a triple nanodisk with equal Co thicknesses.

less than 20 nm, ensuring that the layers were in a single domain state.<sup>18</sup> The MFM investigations of the magnetic states in the multilayer nanomagnets were carried out using a vacuum scanning probe microscope “Solver HV” equipped with a dc electromagnet (manufactured by “NT-MDT”). MFM measurements were performed in the oscillatory non-contact (constant height) mode using home made Co-coated cantilevers. The amplitude of the cantilever oscillations was about 30 nm and the average scanning height was 50–60 nm. The phase shift of the cantilever oscillations caused by the gradient of the magnetic field was registered as the MFM contrast. All measurements were performed in a vacuum of  $10^{-5}$  Torr, which increases the MFM signal due to an increase in the cantilever quality factor.

## RESULTS AND DISCUSSIONS

Experiments performed on trilayer nanomagnets with equal Co thicknesses did not show any signature of a helical state. The MFM image resembled the image of a single uniformly magnetized particle [Fig. 4(a)], which can be explained by peculiarity of the tip-sample interaction; the uppermost layer contributes mostly to the tip-sample interaction, and thus, dominates the MFM contrast. This was also verified by computer modelling. In Fig. 4(b), we illustrate a simulated MFM image for a helical state in a trilayer nanomagnet with equal Co thicknesses.

To clearly verify the noncollinear state in trilayer nanomagnets by MFM, we considered a structure where the thickness of the Co layers increases with increasing distance from the MFM probe. Thus, the change of magnetic moment of the layers was used to compensate for the different distances between the disks and the tip. The calculations showed that a structure with Co layer thicknesses of 16, 11, and 8 nm and with 3 nm spacers has a helical state with  $\theta_{21}=109^\circ$ ,  $\theta_{23}=257^\circ$  and is close to optimal for the MFM observation of the helical state. The model MFM picture calculated for this optimized triple nanodisk is represented in Fig. 5(a). The spiral symmetry of MFM contrast distribution is clearly seen. The experimental MFM image obtained from a nanodisk with Co layer thicknesses of 16, 11, and 8 nm and with 3 nm spacers is presented in Fig. 5(b). As seen in these figures, the experimental MFM contrast distribution is essentially identical to the calculated MFM image.

To realize the noncollinear state, the magnetic energy arising from the shape anisotropy must be smaller than the

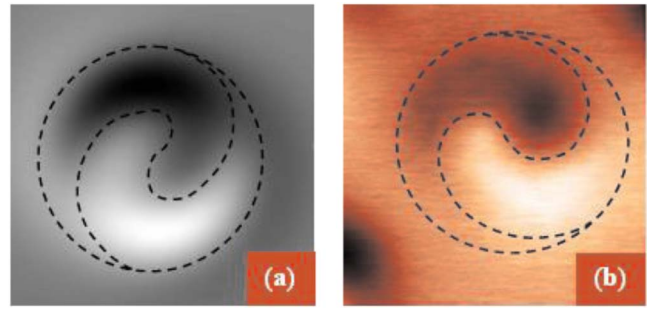


FIG. 5. (Color online) (a) Model MFM contrast distribution for optimized triple nanodisk. (b) Experimental MFM image from triple 16, 11, and 8 nm Co nanodisk. (Frame size  $1 \times 1 \mu\text{m}$ .) The dashed lines separate the regions with dark and bright contrast to emphasize the spiral symmetry of MFM contrast.

magnetostatic interaction, so, the disk ellipticity may not exceed  $0.8 < a/b < 1.2$ , where  $a$  and  $b$  are the lateral dimensions of an elliptical disk.

The left and right helices have equal energies and should therefore be equally probable. Fig. 6 shows a MFM image of two nanomagnets demonstrating the coexistence of left and right handed spiral contrast corresponding to the two helical states with different chirality.

## CONCLUSION

The helical state in artificial multilayer nanomagnets consisting of three single-domain ferromagnetic disks separated by nonmagnetic spacers were investigated by magnetic force microscopy. For optimized trilayer nanomagnets with Co layer thicknesses of 16, 11, and 8 nm and separated by 3 nm Si spacers, the spiral MFM contrast with different chirality was experimentally observed.

The spiral state originates from the competition of magnetostatic interactions between nearest and next nearest neighboring ferromagnetic disks. A spiral state occurs if the

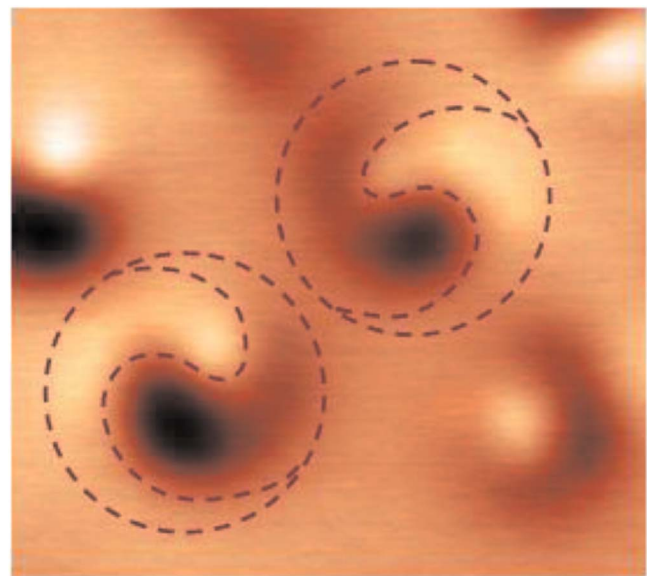


FIG. 6. (Color online) MFM image of two helical nanomagnets with different chirality. The frame size is  $1.8 \times 1.8 \mu\text{m}$ .

energy of magnetostatic interaction between next nearest neighboring disks is sufficiently large compared to the interaction energy of neighboring disks.

The realization of helical nanomagnets is not only of interest for fundamental investigations of nanomagnets. The helical state can be transformed from noncollinear into a noncoplanar cone magnetic spiral by applying an external magnetic field, perpendicular to the ferromagnetic layers. In this case, we expect unusual transport properties along the magnetic field direction.<sup>19–22</sup>

## ACKNOWLEDGMENTS

The authors are very thankful to I. Nefedov, I. Shereshevsky, and C. Binns for assistance and fruitful discussions. This work was partly supported by the RFBR (07-02-01321, 08-02-01202), INTAS (No. 03-51-4778), SFB 491, VR, and by EC through the NANOSPIN project (Contract No. NMP4-CT-2004-013545).

<sup>1</sup>M. N. Baibich, J. M. Broto, A. Fert, F. Nguyen Van Dau, F. Petroff, P. Eitenne, G. Creuzet, A. Friederich, and J. Chazelas, *Phys. Rev. Lett.* **61**, 2472 (1988).

<sup>2</sup>G. Binasch, P. Grünberg, F. Saurenbach, and W. Zinn, *Phys. Rev. B* **39**, 4828 (1989).

<sup>3</sup>M. Jullière, *Phys. Lett.* **54A**, 225 (1975).

<sup>4</sup>J. S. Moodera, L. R. Kinder, T. M. Wong, and R. Meservey, *Phys. Rev. Lett.* **74**, 3273 (1995).

<sup>5</sup>M. Tsoi, A. G. M. Jansen, J. Bass, W.-C. Chiang, M. Seck, V. Tsoi, and P. Wyder, *Phys. Rev. Lett.* **80**, 4281 (1998).

<sup>6</sup>J. Slonczewski, *J. Magn. Magn. Mater.* **159**, L1 (1996).

<sup>7</sup>J. Slonczewski, *J. Magn. Magn. Mater.* **247**, 324 (2002).

<sup>8</sup>M. D. Stiles and A. Zangwill, *J. Appl. Phys.* **91**, 6812 (2002).

<sup>9</sup>A. Kovalev, A. Brataas, and G. E. W. Bauer, *Phys. Rev. B* **66**, 224424 (2002).

<sup>10</sup>G. E. W. Bauer, Y. Tserkovnyak, D. Huertas-Hernando, and A. Brataas, *Phys. Rev. B* **67**, 094421 (2003).

<sup>11</sup>G. E. W. Bauer, Y. Tserkovnyak, D. Huertas-Hernando, and A. Brataas, in *Advances in Solid State Physics*, edited by B. Kramer (Springer-Verlag, Berlin, 2003).

<sup>12</sup>S. Urazhdin, R. Loloee, and W. P. Pratt, Jr., *Phys. Rev. B* **71**, 100401 (2005).

<sup>13</sup>A. Hubert and R. Schäfer, *Magnetic Domains* (Springer, Berlin, 1998).

<sup>14</sup>E. E. Fullerton, J. S. Jiang, and S. D. Bader, *J. Magn. Magn. Mater.* **200**, 392 (1999).

<sup>15</sup>W. C. Koehler, J. W. Cable, M. K. Wilkinson, and E. O. Wollan, *Phys. Rev.* **151**, 414 (1966).

<sup>16</sup>S. J. Jensen and A. R. Mackintosh, *Rare Earth Magnetism: Structures and Excitations* (Oxford University Press, Oxford, 1991).

<sup>17</sup>A. A. Fraerman, S. A. Gusev, L. A. Mazo, I. M. Nefedov, Yu. N. Nozdrin, I. R. Karetnikova, M. V. Sapozhnikov, I. A. Shereshevskii, and L. V. Sukhodoev, *Phys. Rev. B* **65**, 064424 (2002).

<sup>18</sup>R. P. Cowburn, D. K. Koltsov, A. O. Adeyeye, M. E. Welland, and D. M. Tricker, *Phys. Rev. Lett.* **83**, 1042 (1999).

<sup>19</sup>D. Loss, P. Goldbart, and A. V. Balatsky, *Phys. Rev. Lett.* **65**, 1655 (1990).

<sup>20</sup>G. Tatara and H. Kohno, *Phys. Rev. B* **67**, 113316 (2003).

<sup>21</sup>A. A. Fraerman and O. G. Udalov, *Phys. Rev. B* **77**, 094401 (2008).

<sup>22</sup>A. F. Volkov, F. S. Bergeret, and K. B. Efetov, *Phys. Rev. Lett.* **90**, 117006 (2003).